applied sciences

MDPI

Article

Mechanical-Empirical Pavement Design Guide Applied to Portuguese Pavement Structures

Rita Justo-Silva [1], Fábio Simões [1] and Adelino Ferreira [2,*]

[1] Department of Civil Engineering, University of Coimbra, 3030-788 Coimbra, Portugal; ritajustosilva@uc.pt (R.J.-S.); fabiosimoes@uc.pt (F.S.)
[2] Research Centre for Territory, Transports and Environment (CITTA), Department of Civil Engineering, University of Coimbra, 3030-788 Coimbra, Portugal
* Correspondence: adelino@dec.uc.pt

Abstract: This paper describes the characteristics of the new pavement design method developed by the American Association of State Highway and Transportation Officials (AASHTO), known as AASHTOWare Pavement-ME®, and presents the results of its application to the flexible pavement structures presented in the Portuguese Manual of Pavement Structures for the national road network. The results obtained clearly show that it is a very useful tool for road engineers not only for designing new pavement structures but also for the analysis of their performance and for efficiently planning maintenance and rehabilitation interventions. According to the characteristics of the case study that was considered, rutting is the most critical distress, since it presents values close to its threshold value of 20.0 mm, a value that is defined in Portuguese Quality Control Plans.

Keywords: pavement design; deterministic pavement performance prediction models; mechanistic empirical model; international roughness index; rutting; cracking

Citation: Justo-Silva, R.; Simões, F.; Ferreira, A. Mechanical-Empirical Pavement Design Guide Applied to Portuguese Pavement Structures. *Appl. Sci.* **2022**, *12*, 5656. https://doi.org/10.3390/app12115656

Academic Editors: Jiaqi Chen, Kezhen Yan and Jun Xie

Received: 3 May 2022
Accepted: 31 May 2022
Published: 2 June 2022

1. Introduction

With the objective of improving pavement design from an empirical approach to a mechanistic-empirical approach, by including pavement mechanistic behavior, aiming to correlate applied loads and observed distresses [1], the American Association of State Highway and Transportation Officials (AASHTO) developed a new pavement design method called the Mechanistic Empirical Pavement Design Guide—MEPDG [2] to replace the previous pavement design method of 1993 [3]. The MEPDG is a mechanistic-empirical pavement design method in which pavement performance is predicted using the pavement's structural response in terms of the following pavement performance indicators: (1) rutting; (2) international roughness index (IRI); (3) fatigue cracking; (4) transverse cracking; and (5) alligator cracking.

A software package has been developed and made available to the pavement design community that allows the calibration and application of this new pavement design method in different countries and regions subject to different traffic, climate, and pavement foundation conditions. Initially, the pavement design method requests data input related to traffic, climate, materials, and pavement structure. The pavement performance indicators mentioned above are then calculated and presented for further analysis considering threshold values which have been established, for example, in highway public–private partnership contracts.

This new pavement design method has three hierarchical levels for the input variables, including climate, traffic loading, layer structure, and material properties, which define the accuracy of the data according to three levels: level 1; level 2; and level 3. In general, the level 1 input is the most accurate value that it is possible to obtain for a certain input. This usually represents site specific measurements and laboratory data. Contrary to the previous level, level 3 input is either the default value used in the AASHTOWare Pavement-ME®

or a nominal value provided by a local agency. This requires the least amount of data, considering default values established according to the characteristics of the region where the road will be built. Level 2 input is estimated from correlations or regression equations.

In recent years, several research studies, usually supported by road agencies, have been undertaken to evaluate the application of this new pavement design method. Ng et al. [4] presented the results of a comprehensive test program to calibrate the MEPDG for the state of Wyoming, consisting of field data collection and laboratory soil tests. They concluded that the results of the test program facilitated the implementation of the MEPDG. There are several documents in the literature that can be used for regional or local calibration of the MEPDG [5,6]. Jannat et al. [7] presented the results of the application of the MEPDG procedure to pavements of provincial highways of Ontario, Canada. A regression analysis was carried out for calibrating the rutting and IRI models by comparing the predicted distress to the observed distress. The results demonstrated that whereas the MEPDG provided a fairly unbiased prediction of the IRI value, it often over-predicted the total rutting. Jannat and Tighe [8] presented the results of a sensitivity analysis to the inputs of MEPDG distresses to identify the effect of the accuracy level of inputs based on experimental design.

Saha et al. [9] compared the Alberta Transportation Pavement Design (ATPD) procedure with the MEPDG procedure to explore the possibility of MEPDG implementation for pavement design in Alberta, Canada. The ATPD pavement design method is based mainly on the AASHTO 1993 guide, with minor modifications regarding the asphalt concrete mix design, the structural layer coefficients, and design reliability levels. Six different design cases were defined with three different traffic levels and two different subgrade materials. The ATPD design thicknesses were used in the MEPDG for each case to predict the pavement performance reliabilities at the end of the 20-year design life. It was found that, when using the MEPDG, only the cases with a strong subgrade material and a low level of traffic met the default limit value for total pavement rutting. On the other hand, all sections failed due to excessive IRI values. Saha et al. [10] continued later with another study to investigate the quality of the recently developed Canadian climatic database and the effect of climatic factors on flexible pavement performance using the MEPDG procedure. It was found that total pavement rutting and IRI showed sensitivity to climate changes.

Nassiri et al. [11] used the installed weigh-in-motion (WIM) systems at six highway locations to characterize traffic loads in Alberta for the MEPDG design. Seasonal and regional trends in traffic characteristics of the six WIM sites were investigated and compared with the default values in the MEPDG for two years. Truck traffic classification (TTC) and axle load distribution factor (ALDF) for the WIM sites showed deviations from the MEPDG defaults. Seasonal variations were also evident in the distribution of different classes of trucks throughout the year. Differences were attributed to cold climate conditions and special truck traffic in Alberta due to local industries. It was also found that the performance of flexible pavements was sensitive to TTC and ALDF. El-Badawy et al. [12] studied the development of traffic characteristics to facilitate the implementation of the MEPDG procedure in Idaho. Classification and weight data were collected at 25 WIM sites, but only 12 sites were found to have complete and accurate data. Predicted distresses and IRI values for a typical pavement section and traffic data obtained at the investigated WIM sites (level 1) were compared to predicted distresses/IRI using statewide/national (level 3) default traffic inputs. This comparison revealed that site-specific axle load spectra (ALS), vehicle class distribution factors (VCDF), and monthly adjustment factors (MAF) had a significant impact on longitudinal cracking. Statewide ALS yielded high differences in alligator cracking predictions, while statewide MAF and VCDF yielded only moderate differences compared to site-specific ALS. Very low prediction differences occurred in rutting when statewide/national default ALS, MAF, and VCDF were used as opposed to site-specific data. Furthermore, the level of input of the investigated traffic parameters was found not to affect IRI. Finally, they concluded that the statewide/national number of axles per truck could be used instead of site-specific values without sacrificing the accuracy of the pavement performance predictions. Wu et al. [13] presented a study on using the MEPDG design software to evaluate the performance of typical Louisiana flexible pavement structures and compared it to the existing pavement performance data available in the Louisiana Pavement Management System. The results of the comparison between the measured and predicted pavement distresses showed a strong dependency on the type of pavement structure considered in the study. In general, the MEPDG rutting models tended to overpredict the total rutting for Louisiana's flexible pavements, whereas both fatigue cracking and IRI models in the MEPDG seemed to be adequate for most of the selected projects.

The literature comprises other studies related to the evaluation of the MEPDG application [14–18]. However, to the best of our knowledge, none of them addresses the application of the MEPDG procedure to a complete country's catalogue of pavement structures. This paper presents and discusses the results of the application of the MEPDG procedure to the flexible pavement structures presented in the Portuguese Manual of Pavement Structures for the national road network [19]. It was demonstrated that it can be quite useful for road agencies that need to know the value of each pavement performance indicator during the complete pavement life to carry out the objectives defined in concession contracts as well as in Quality Control Plans.

2. The MEPDG Design Methodology

2.1. Introduction

The MEPDG design methodology comprises three main phases as shown in Figure 1. The first phase, named Evaluation, consists of inserting all the data into the MEPDG software and is followed by the Analysis (second phase). Finally, the Strategy Selection is the last phase and corresponds to the selection of the best alternative that complies with all requirements. The input data required for the MEPDG software are the information about the traffic, the climate, the pavement structure, and the properties of the materials, which will be briefly explained in the following subsections.

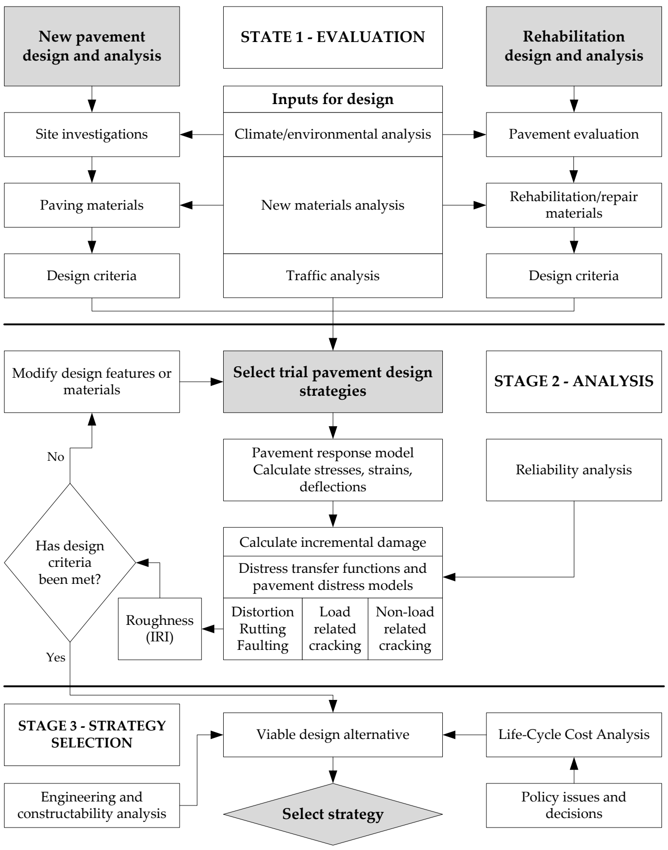

Figure 1. MEPDG design methodology [3].

2.2. Traffic

While the AASHTO 1993 pavement design methodology requires the number of 18-kips Equivalent Single Axle Load (ESAL) as the only traffic input, the MEPDG requires four main traffic inputs for the design of pavement structures [3,20,21]: (1) base year truck traffic volume; (2) traffic volume adjustment factors; (3) axle load distribution factors; and (4) general traffic inputs. The traffic volume adjustment factors are used to adjust the base year traffic volume. These adjustment factors are the monthly adjustment factors (MAF), vehicle class distribution (VCD), hourly truck distribution (HTD), and traffic growth factors. The general traffic input data include the number of axles per truck, axle configuration, tire pressure, traffic wander, and wheel base. The MEPDG considers 10 different vehicle classes, ranging from class 4 to class 13 as presented in Figure 2.

In Portugal, traffic classes are not equal to the traffic classes presented in Figure 2. There are 11 classes, ranging from A to K [22]: classes A and B correspond to bicycles; class C corresponds to motorcycles; classes D and E correspond to cars; and the remaining classes (F, G, H, I, J, and K) correspond to trucks. For to this reason, detailed traffic data are required to convert the 6 classes of trucks considered in Portugal into the 10 classes considered in the MEPDG. In Portugal, there is not enough information to achieve level 1; however, using all the available information, level 2 can be achieved. Level 1 requires, for example, axle load spectra (ALS), also called axle load distribution factors, which can only be determined from WIM data.

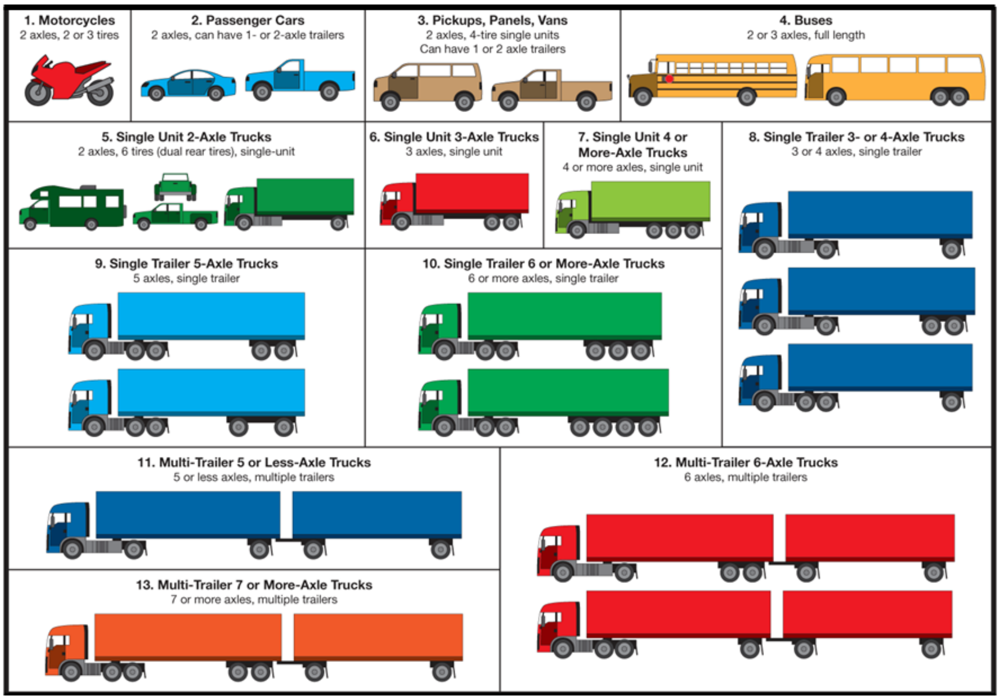

Figure 2. Traffic classes considered by MEPDG [23,24].

2.3. Climate

The MEPDG software is linked to the Enhanced Integrated Climatic Model (EICM) to include the effects of environmental conditions on pavement performance [3,25–27]. The EICM uses data from climatic files containing hourly ambient temperature and relative humidity, precipitation, sunshine percentage, and wind speed. The EICM is used to predict the temperature profile throughout the pavement depth together with the moisture content and freezing conditions in the unbound layers. The predicted temperature in flexible pavements is directly related to the stiffness of the asphalt concrete layers and, therefore, is indispensable for predicting thermal cracking and rutting.

There are 850 weather stations in the USA that collect all the necessary data in the format used by the MEPDG software [17]. The Transportation Association of Canada has also implemented the MEPDG using accurate climatic data from 220 weather stations across Canada, which provided different values of pavement performance indicators for each province [10].

In Portugal, the weather stations do not collect the required data in the format used by the MEPDG software. Therefore, it was necessary to collect and organize all the climate data provided by the Portuguese Institute of the Sea and Atmosphere.

The climatic ICM file consists of one line for each day (Table 1) containing information related to month, day, year, hour of sunrise, hour of sunset, and daily solar radiation. Below this line, there are 24 lines, each one corresponding to one hour of the same day. These lines have the information indicated in the following order: hour; temperature in Fahrenheit; precipitation in inches; wind speed in miles per hour; the percentage of the sun or cloudiness level; and the hourly groundwater depth in feet. A climate ICM file was prepared for the Coimbra region with two years of climate data.

Table 1. Part of the climate data file for the Coimbra region.

Month	**Day**	**Year**	**Sunrise**	**Sunset**	**Solar Radiation**
5	6	2018	6.56667	20.5500	3548.76
Hour	**Temperature (°F)**	**Precipitation (in)**	**Wind speed (mph)**	**Clear sky (%)**	**Depth of the groundwater level (ft)**
0	55.4	0.00	1.6	100	50
1	54.5	0.00	0.7	100	50
...	...	...	...	...	...
23	57.7	0.02	0.2	0	50
...	...	...	...	...	...

2.4. Pavement Structure and Material Properties

Finally, the last data input into MEPDG software are the pavement structure and the properties of the materials. As for traffic data, there are also 3 levels that define the accuracy of these data. First, it is necessary to introduce the characteristics of the pavement structure, i.e., the number of layers; type of material for each layer; and layer thickness. The data referring to the material properties required for each layer are different for asphalt and granular layers. For asphalt layers, the software requires the aggregate gradation, the characteristics of the asphalt binder, the reference temperature, the Poisson's ratio, the effective binder content, the air voids, the total unit weight, and the thermal properties. For granular layers, the aggregate gradation distribution, the California Bearing Ratio (CBR), the coefficient of lateral pressure, and the Poisson's ratio are required.

2.5. Pavement Performance Prediction Models

The pavement performance prediction models used by the MEPDG software to predict the value of each pavement performance indicator (i.e., longitudinal cracking, alligator cracking, AC rutting, total rutting, and IRI) are presented in Appendix A [3]. Global calibration factors were considered in this study. These pavement performance prediction models were defined for application at project-level, but they have also great potential, for example, for application at network-level in Pavement Management Systems [28–30] and Road Safety Management Systems [31,32].

3. Application of MEPDG to the Portuguese Pavement Structures

3.1. Introduction

The MEPDG software was applied to the pavement structures recommended in the Portuguese Manual of Pavement Structures for the national road network [19]. Figure 3 presents the characteristics of the 16 different pavement structures (e.g., thickness, stiffness modulus, Poisson's ratio, and type of material) ordered according to their structural number [33–35]. These pavement structures were defined using the Shell pavement design method [36] considering an accumulated damage between 80% and 100%, with an additional verification performed with the University of Nottingham [37] and Asphalt Institute [38] pavement design methods.

	Flexible pavement structures															
	P1	**P2**	**P3**	**P4**	**P5**	**P6**	**P7**	**P8**	**P9**	**P10**	**P11**	**P12**	**P13**	**P14**	**P15**	**P16**
Thickness (cm)	4	4	4	4	5	5	4	5	5	6	5	6	5	6	6	6
Stiffness Mod. (MPa)	4000	4000	4000	4000	4000	4000	4000	4000	4000	4000	4000	4000	4000	4000	4000	4000
Poisson's ratio	0.35	0.35	0.35	0.35	0.35	0.35	0.35	0.35	0.35	0.35	0.35	0.35	0.35	0.35	0.35	0.35
Thickness (cm)	6	8	12	14	14	16	18	17	19	18	20	20	23	22	24	26
Stiffness Mod. (MPa)	4000	4000	4000	4000	4000	4000	4000	4000	4000	4000	4000	4000	4000	4000	4000	4000
Poisson's ratio	0.35	0.35	0.35	0.35	0.35	0.35	0.35	0.35	0.35	0.35	0.35	0.35	0.35	0.35	0.35	0.35
Thickness (cm)	20	20	20	20	20	20	20	20	20	20	20	20	20	20	20	20
Stiffness Mod. (MPa)	200	200	200	200	200	200	200	200	200	200	200	200	200	200	200	200
Poisson's ratio	0.35	0.35	0.35	0.35	0.35	0.35	0.35	0.35	0.35	0.35	0.35	0.35	0.35	0.35	0.35	0.35
HMA thickness (cm)	10	12	16	18	19	21	22	22	24	24	25	26	28	28	30	32
Structural Number (SN)	2.36228	2.63000	3.16544	3.43316	3.60639	3.87411	3.96860	4.00797	4.27569	4.31506	4.40955	4.58278	4.81113	4.85050	5.11822	5.38594

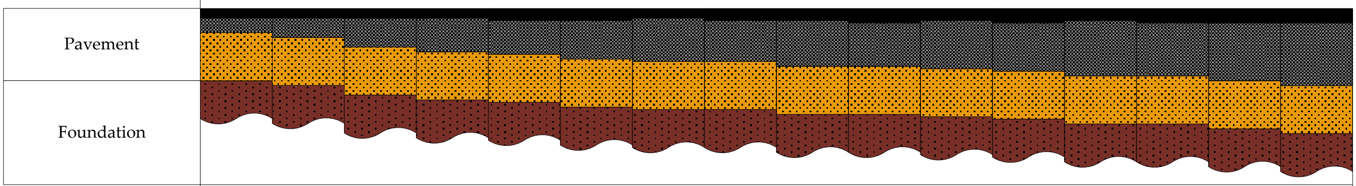

Key: HMA – Hot Mix Asphalt.

Figure 3. Characteristics of pavement structures (adapted from [35]).

The Portuguese manual presents the 16 different flexible pavement structures for each combination between traffic and pavement foundation classes (Table 2). Each pavement foundation class corresponds to a stiffness modulus value. They are as follows: (1) 30 MPa for class F1; (2) 60 MPa for class F2; (3) 100 MPa for class F3; and (4) 150 MPa for class F4. No flexible pavement structures were defined for pavement foundation class F1 because, according to the Portuguese manual, this type of pavement foundation is not adequate for a flexible pavement with an asphalt base layer.

The Portuguese manual [19] contains most of the data required by the MEPDG software, such as, for example, the percentage of the effective binder content and the air voids defined according to the type of layer and material. There are also minimum and maximum limit values for the effective binder content and the porosity, depending on the type of layer and material. The traffic data are also specified by the Portuguese manual, including the Average Annual Daily Truck Traffic (AADTT). Nevertheless, the Portuguese Road Network Agency (Infraestruturas de Portugal) has detailed traffic data for each segment of the national road network [39].

Table 3 presents the threshold for each pavement performance indicator considered in this case study. The IRI has three different thresholds, which depend on the percentage of the total length of the project. These thresholds were based on Portuguese specifications [40], Portuguese Quality Control Plans (QCP), and pavement design practice. Within the scope of road concession contracts [41], the concessionaires need to submit to the Portuguese Institute of Mobility and Transports (IMT) a Quality Control Plan (QCP) and a Maintenance and Operation Manual (MOM). The QCP presents the thresholds for each pavement performance indicator that a highway concessionaire needs to fulfill in each year of the concession period, which is usually 30 years. Contractual infractions are penalized with fines, in which the global sum varies according to its gravity between EUR 5000 and EUR 100,000 or daily values that can vary between EUR 500 and EUR 5000.

Table 2. Pavement structure for each combination of traffic and foundation.

Traffic					Foundation		Pavement
Class	AADTT	Traffic Growth Rate	Truck Factor	Heavy Trucks (20 Years)	Class	E (MPa)	Class
T_6	150	3%	2	1.47×10^6	F_2	60	P_3
	150	3%	2	1.47×10^6	F_3	100	P_2
	150	3%	2	1.47×10^6	F_4	150	P_1
T_5	300	3%	3	2.94×10^6	F_2	60	P_7
	300	3%	3	2.94×10^6	F_3	100	P_4
	300	3%	3	2.94×10^6	F_4	150	P_3
T_4	500	4%	4	5.44×10^6	F_2	60	P_{11}
	500	4%	4	5.44×10^6	F_3	100	P_6
	500	4%	4	5.44×10^6	F_4	150	P_5
T_3	800	4%	4.5	8.70×10^6	F_2	60	P_{13}
	800	4%	4.5	8.70×10^6	F_3	100	P_9
	800	4%	4.5	8.70×10^6	F_4	150	P_8
T_2	1200	5%	5	1.45×10^7	F_2	60	P_{15}
	1200	5%	5	1.45×10^7	F_3	100	P_{12}
	1200	5%	5	1.45×10^7	F_4	150	P_{10}
T_1	2000	5%	5.5	2.42×10^7	F_2	60	P_{16}
	2000	5%	5.5	2.42×10^7	F_3	100	P_{14}
	2000	5%	5.5	2.42×10^7	F_4	150	P_{12}

Table 3. Pavement performance indicator thresholds.

Longitudinal Cracking (m/km)	Alligator Cracking (%)	AC Rutting (mm)	Total Rutting (mm)	IRI (mm/km)
200	20	15	20	2000 (in 50% of the length) 3000 (in 80% of the length) 3500 (in 100% of the length)

3.2. Results

The application of the MEPDG software produces a file with all the input data and results of the evolution of each pavement performance indicator along with the entire design life of 20 years. Table 4 presents the predicted values for each pavement performance indicator (i.e., longitudinal cracking, alligator cracking, AC rutting, total rutting, and IRI) corresponding to each combination of traffic class, pavement foundation class, and pavement structure. Figures 4–8 show the predicted values for each pavement performance indicator in each year of the design life.

The pavement structures recommended by the Portuguese manual were defined using the Shell pavement design method considering an accumulated damage between 80% and 100%, with an additional verification performed with the University of Nottingham and Asphalt Institute pavement design methods. Therefore, using the MEPDG, it would be reasonable to expect values in the same range (i.e., between 80% and 100%) for at least one of the following pavement performance indicators: alligator cracking (bottom-up fatigue) or total rutting (permanent deformation). For the other pavement performance indicators, only small variations would be expected, because each pavement was designed for a specific combination of traffic and pavement foundation.

Table 4. Prediction values for the pavement performance indicators.

Traffic Class	Foundation Class	Pavement Class	Longitudinal Cracking (m/km)	Alligator Cracking (%)	AC Rutting (mm)	Total Rutting (mm)	IRI (mm/km)
T_6	F_2	P_3	14.1	0.81	5.1	12.1	1578
	F_3	P_2	23.9	2.11	5.8	12.0	1591
	F_4	P_1	16.0	2.91	5.9	11.5	1589
T_5	F_2	P_7	4.6	0.40	7.1	13.4	1605
	F_3	P_4	23.1	0.82	7.6	12.8	1594
	F_4	P_3	29.4	1.16	7.7	12.2	1583
T_4	F_2	P_{11}	3.0	0.41	9.1	15.2	1651
	F_3	P_6	24.4	0.78	10.8	15.8	1670
	F_4	P_5	40.7	1.05	11.3	15.5	1665
T_3	F_2	P_{13}	1.8	0.38	10.8	16.7	1687
	F_3	P_9	16.8	0.64	12.5	17.3	1705
	F_4	P_8	36.4	0.82	13.3	17.3	1706
T_2	F_2	P_{15}	1.0	0.43	9.9	15.8	1665
	F_3	P_{12}	11.2	0.79	10.7	16.3	1689
	F_4	P_{10}	33.9	0.98	12.4	17.0	1718
T_1	F_2	P_{16}	1.1	0.52	11.2	17.0	1697
	F_3	P_{14}	11.9	0.76	14.5	19.1	1750
	F_4	P_{12}	35.4	0.90	15.8	19.7	1765

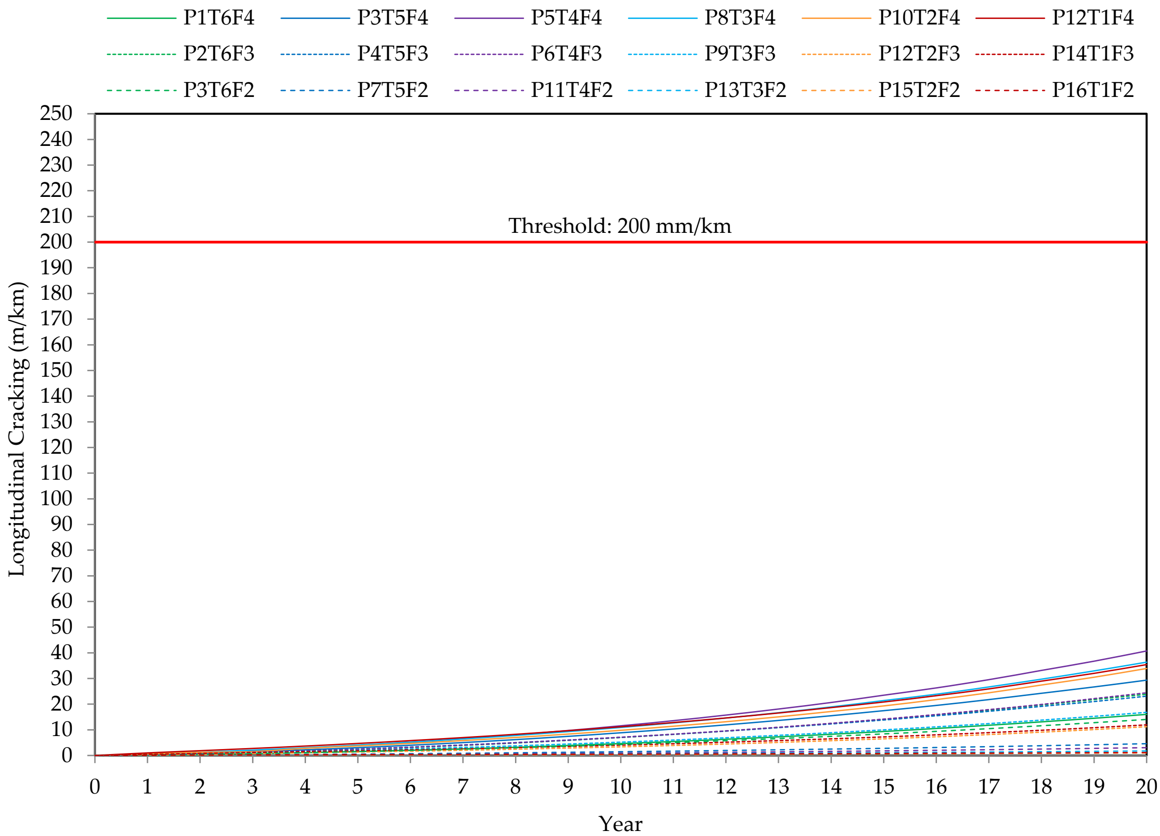

Figure 4. Evolution of longitudinal cracking during the design life.

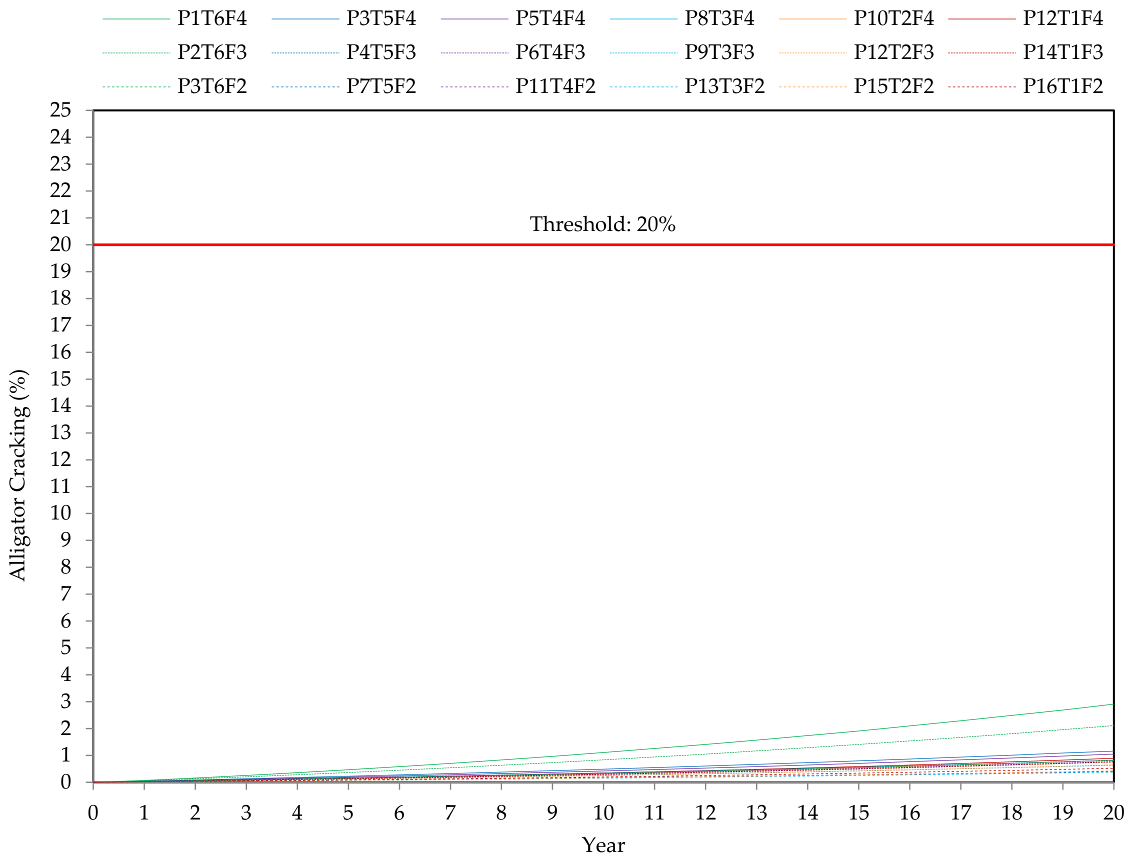

Figure 5. Evolution of alligator cracking during the design life.

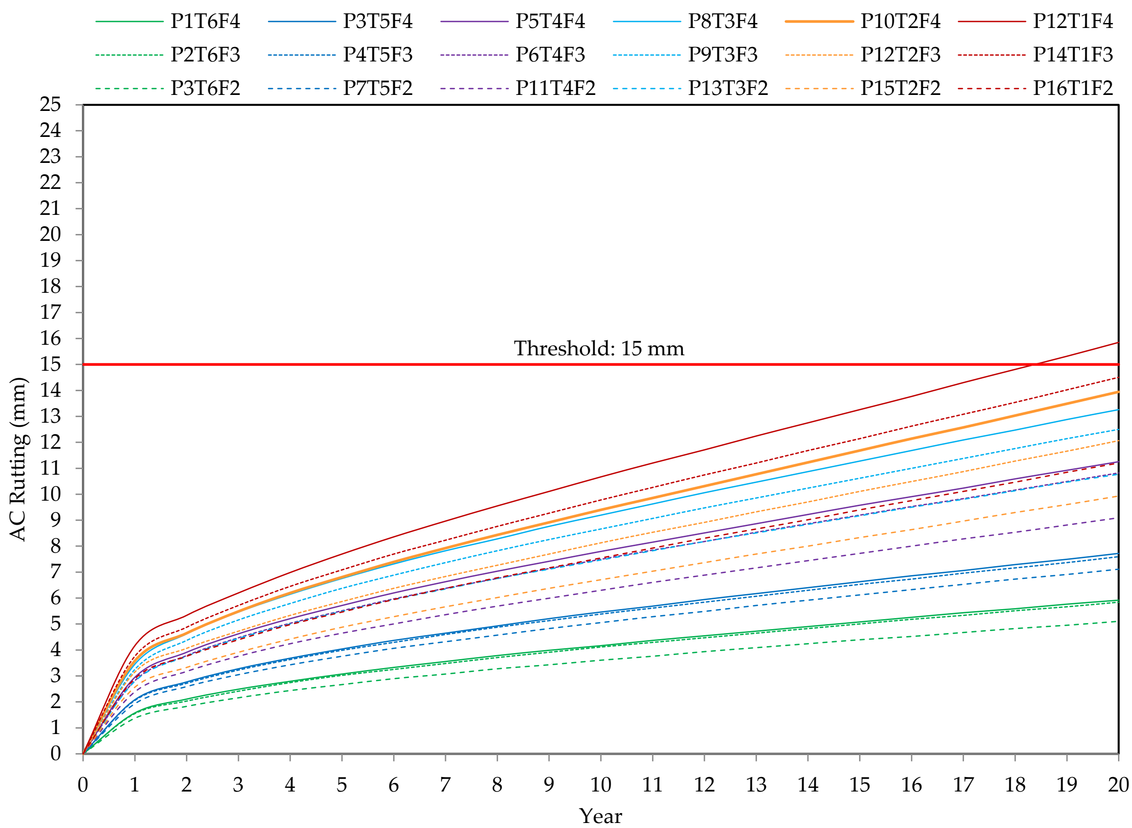

Figure 6. Evolution of rutting in AC layers during the design life.

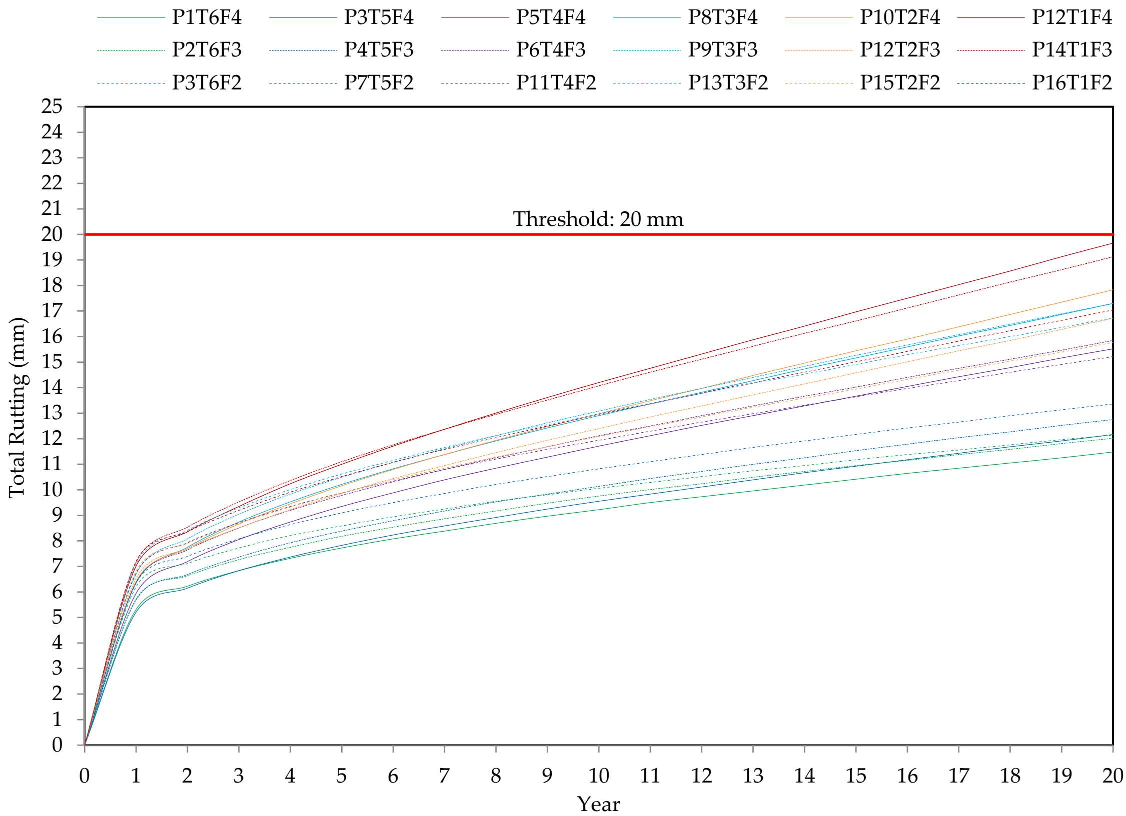

Figure 7. Evolution of total rutting during the design life.

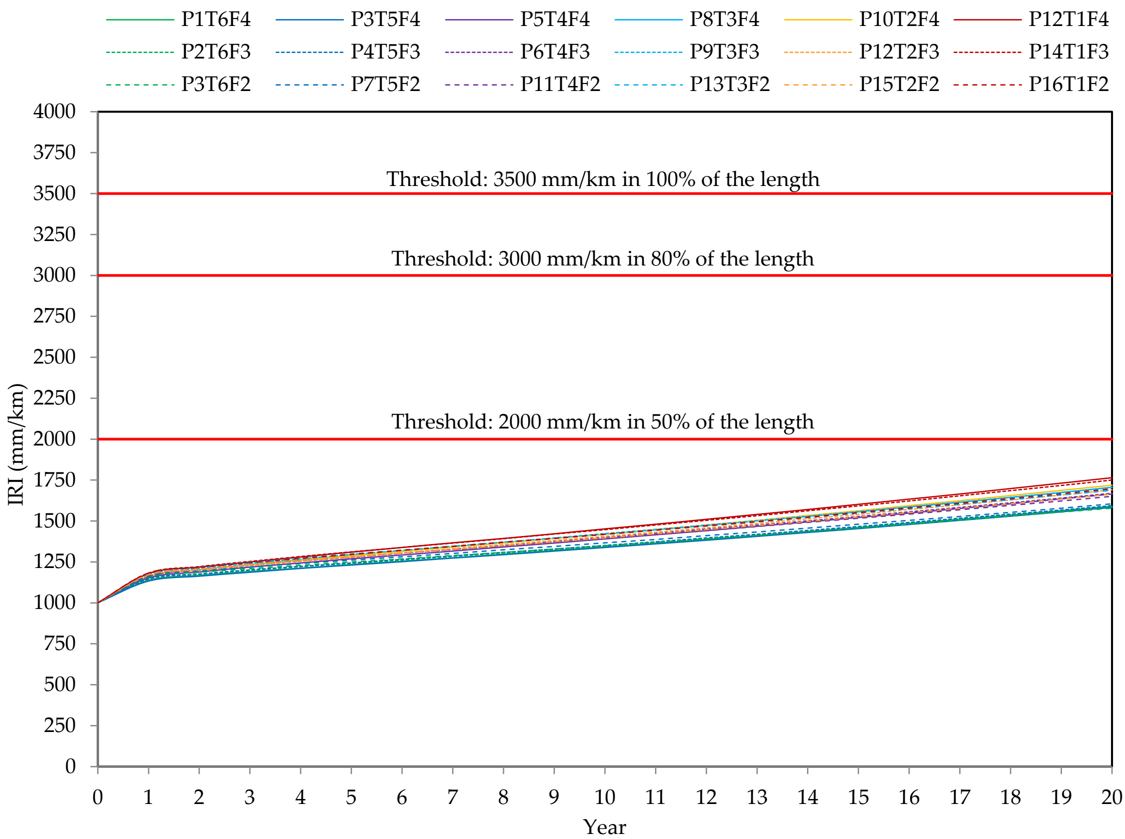

Figure 8. Evolution of IRI during the design life.

Analyzing Table 4 and Figure 4, one can see that there is a small variation in the longitudinal cracking (top-down fatigue) at the end of the design life of 20 years. More specifically, it ranged from 1.0 to 40.7 m/km, which corresponded to combinations $P_{15}T_2F_2$ and $P_5T_4F_4$, respectively. This variation occurred essentially by changing the foundation class within the same traffic class. The only exception was the variation of the longitudinal cracking value for traffic class T_6, which ranged only between 14.1 and 23.9 m/km. One can also see that the longitudinal cracking values were quite far from the threshold value of 200 m/km for the whole design life.

Regarding the alligator cracking (bottom-up fatigue), the analysis of Table 4 and Figure 5 reveals a very small variation (0.38% to 2.91%) at the end of the design life, which corresponded to combinations $P_{13}T_3F_2$ and $P_1T_6F_4$, respectively. Nevertheless, this very small variation continued to occur when changing the foundation class from F_2 to F_3 and to F_4, within the same traffic class. Finally, it is worth mentioning that the alligator cracking values were quite far from the threshold value of 20% for the whole design life.

As far as rutting is concerned, the variation in AC rutting (contribution of asphalt concrete layers only) was greater than the variation in total rutting (permanent deformation), as suggested by Table 4 and Figures 6 and 7. There was a large variation in the AC rutting, ranging from 5.1 to 15.8 mm at the end of the design life, which corresponded to combinations $P_3T_6F_2$ and $P_{12}T_1F_4$, respectively, exceeding the threshold of 15.0 mm in only one situation, i.e., pavement structure P_{12}. This is the pavement structure recommended in the Portuguese manual for the combination of traffic class T_1 and pavement foundation F_4. Total rutting varied between 11.5 and 19.7 mm, corresponding to combinations $P_1T_6F_4$ and $P_{12}T_1F_4$, respectively, not exceeding the threshold of 20.0 mm in any situation. The maximum AC rutting and maximum total rutting were verified for the same combination $P_{12}T_1F_4$. It can also be observed that the variation of AC rutting and total rutting was small within the same traffic class.

Finally, Table 4 and Figure 8 show a very small variation in IRI, ranging from 1578 to 1847 mm/km at the end of the design life, which corresponded to combinations $P_3T_6F_2$ and $P_{10}T_2F_4$, respectively. Therefore, the IRI was the pavement performance indicator with the most homogeneous results for all the pavement structures recommended in the Portuguese manual for each combination of traffic and pavement foundation. Furthermore, the IRI values were found to be much lower than the threshold value of 3500 mm/km (for 100% of the length of the project) but were close to the threshold value of 2000 mm/km (for 50% of the length of the project).

Those results are particularly relevant within a context where increasing attention has been paid to the excessive contribution of the road transportation mode to the greenhouse gases (GHGs) emissions [42]. Vehicle energy consumption and emissions are strongly affected by pavement surface characteristics due to a phenomenon known as rolling resistance. Among the pavement surface properties influencing rolling resistance, pavement roughness plays a prominent role. Given the long service life of pavements and the potentially high volume of traffic they carry, ensuring that pavement roughness, as measured by IRI, remains low over time is of supreme importance to mitigate and reduce the impacts of the road transport mode on climate change. To summarize, by using the MEPDG, values in the range of 80% and 100% of the threshold values would be expected for at least one of the following pavement performance indicators: alligator cracking (bottom-up fatigue) or total rutting (permanent deformation). However, when analyzing the results presented in Table 4, it can be seen that this was neither the case for these pavement performance indicators nor for the others. The pavement performance indicator closest to this situation was total rutting. These results demonstrate that by applying the MEPDG design method to the Portuguese conditions, the most critical distress is total rutting, since it presented values close to its threshold, i.e., 20.0 mm.

4. Conclusions

The Shell pavement design method has been used widely in Portugal. The Portuguese Manual of Pavement Structures for the national road network is a user-friendly document used to define a road pavement structure considering data for traffic, climate, pavement foundation, and material properties. In terms of pavement maintenance management or pavement performance prediction using indicators such as longitudinal cracking, alligator cracking, rutting, IRI, etc., neither the Shell pavement design method nor the Portuguese manual can greatly assist road agencies. However, the new pavement design method developed by AASHTO, known as AASHTOWare Pavement-ME®, can be quite useful for road agencies that need to know the value of each pavement performance indicator during the complete pavement life in order to plan maintenance and rehabilitation interventions. Consequently, it will be possible to carry out the objectives defined in concession contracts as well as in Quality Control Plans. However, the application of this new pavement design method requires a large quantity of data, essentially about traffic, climate, and materials properties, which must be collected and organized in files with specific formats.

The new AASHTO pavement design method was developed to become a reference method worldwide. Apart from academic purposes, it is expected that road agencies and road pavement designers from many countries across the world will begin to use this new pavement design method. Several different types of analysis should be performed, varying traffic data, material properties, and application in various regions with different climatic data, to define, for example, the pavement performance indicators that are critical in each region of the country. An economic analysis of pavement structures, including construction costs, maintenance and rehabilitation costs, user costs, and the residual value of pavements, should also be made to optimize the pavement structure for new roads or the overlay thickness for deteriorated roads. Likewise, it is important to estimate the potential environmental impacts related to the complete lifecycle of the pavement structures.

Future developments on this subject include regional or local calibration, considering regression analyses between the predicted and observed pavement distresses stored in the Portuguese Pavement Management Systems, i.e., cracking, rutting, and IRI. This is an important step for a Portuguese road agency before starting to use officially the new AASHTO mechanistic-empirical pavement design guide to define the pavement structures for the national and municipal road network. Another important future development is to use these pavement performance prediction models for application at network-level in Pavement Management Systems and also in Road Safety Management Systems.

Author Contributions: Conceptualization and methodology, A.F.; data curation, R.J.-S., F.S. and A.F.; formal analysis, R.J.-S., F.S. and A.F.; funding acquisition, A.F.; investigation, R.J.-S., F.S. and A.F.; project administration, A.F.; supervision, A.F.; validation, R.J.-S., F.S. and A.F.; writing—original draft, R.J.-S. and A.F.; writing—review and editing, A.F. All authors have read and agreed to the published version of the manuscript.

Funding: This research work was carried out in the framework of project PAVENERGY-Pavement Energy Harvest Solutions (PTDC/ECM-TRA/3423/2014), co-financed by the European Regional Development Fund (POCI-01-0145-FEDER-016676) through the Operational Program for Competitiveness Factors (COMPETE) and by national funds through the Portuguese Foundation for Science and Technology (FCT).

Acknowledgments: The author Rita Justo-Silva is grateful to the Portuguese Foundation for Science and Technology for her MIT-Portugal Ph.D. Grant (PD/BD/113721/2015).

Conflicts of Interest: The authors declare no conflict of interest.

Appendix A

Appendix A.1. Pavement Performance Prediction Models

Appendix A.1.1. Longitudinal Cracking and Alligator Cracking

$$N_{f-HMA} = k_{f1}(C)(C_H)\beta_{f1}(\varepsilon_t)^{k_{f2}\beta_{f2}}(E_{HMA})^{k_{f3}\beta_{f3}} \tag{A1}$$

$$C = 10^M \tag{A2}$$

$$M = 4.84\left(\frac{V_{be}}{V_a + V_{be}} - 0.69\right) \tag{A3}$$

For longitudinal cracking (top-down cracking)

$$C_H = \frac{1}{0.01 + \frac{12.00}{1+e^{(15.676-2.8186H_{HMA})}}} \tag{A4}$$

For alligator cracking (bottom-up cracking)

$$C_H = \frac{1}{0.000398 + \frac{0.003602}{1+e^{(11.02-3.49H_{HMA})}}} \tag{A5}$$

$$DI = \sum(\Delta DI)_{j,m,l,p,T} = \sum\left(\frac{n}{N_{f-HMA}}\right)_{j,m,l,p,T} \tag{A6}$$

$$FC_{Bottom} = \left(\frac{1}{60}\right)\left(\frac{C_4}{1 + e^{(C_1C_1^* + C_2C_2^* Log(DI_{Bottom} \times 100))}}\right) \tag{A7}$$

$$C_1^* = -2C_2^* \tag{A8}$$

$$C_2^* = -2.40874 - 39.748(1 + H_{HMA})^{-2.856} \tag{A9}$$

$$FC_{Top} = 10.56\left(\frac{C_4}{1 + e^{(C_1 - C_2 Log(DI_{Top}))}}\right) \tag{A10}$$

where

N_{f-HMA} is the allowable number of axle-load applications for a flexible pavement and HMA overlays;

ε_t is the tensile strain at critical locations and calculated by the structural response model (in/in);

E_{HMA} is the dynamic modulus of the HMA measured in compression (psi);

k_{f1}, k_{f2}, k_{f3} are global field calibration parameters (from the NCHRP 1-40D recalibration) ($k_{f1} = 0.007566$, $k_{f2} = -3.9492$ and $k_{f3} = -1.281$);

$\beta_{f1}, \beta_{f2}, \beta_{f3}$ are local or mixture field calibration constants; for the global calibration, these constants were all set to 1.0;

V_{be} is the effective asphalt content by volume (%);

V_a is the percent of air voids in the HMA mixture;

C_H is the thickness correction term, dependent on the type of cracking;

H_{HMA} is the total HMA thickness (in);

DI is the cumulative damage index;

n is the actual number of axle-load applications within a specific period of time;

j is the axle-load interval;

m is the axle-load type (single, tandem, tridem, quad, or special axle configuration;

l is the truck type using the truck classification groups included in the MEPDG;

p is the month;

T is the median temperature for the five temperature intervals or quintiles used to subdivide each month (°F);

FC_{Bottom} is the area of alligator cracking that initiates at the bottom of the HMA layers (% of total lane area);

DI_{Bottom} is the cumulative damage index at the bottom of the HMA layers;

$C_{1,2,4}$ are the transfer function regression constants ($C_4 = 6000$; $C_1 = 1.00$; $C_2 = 1.00$);

FC_{Top} is the length of the longitudinal cracks that initiate at the top of the HMA layer (ft/mi);

DI_{Top} is the cumulative damage index near the top of the HMA surface;

$C_{1,2,4}$ are the transfer function regression constants ($C_1 = 7.00$; $C_2 = 3.5$; $C_4 = 1000$).

Appendix A.1.2. Rutting in HMA Pavement Layers

$$\Delta_{p(HMA)} = \varepsilon_{p(HMA)} h_{HMA} = \beta_{1r} k_z \varepsilon_{r(HMA)} 10^{k_{1r}} n^{k_{2r}\beta_{2r}} T^{k_{3r}\beta_{3r}} \tag{A11}$$

$$k_z = (C_1 + C_2 D) 0.328196^D \tag{A12}$$

$$C_1 = -0.1039(H_{HMA})^2 + 2.4868 H_{HMA} - 17.342 \tag{A13}$$

$$C_2 = 0.0172(H_{HMA})^2 - 1.7331 H_{HMA} + 27.428 \tag{A14}$$

where

$\Delta_{p(HMA)}$ is the accumulated permanent or plastic vertical deformation in the HMA layer (in);

$\varepsilon_{p(HMA)}$ is the accumulated permanent or plastic axial strain in the HMA layer (in/in);

$\varepsilon_{r(HMA)}$ is the resilient or elastic strain calculated by the structural response model at the mid-depth of each HMA layer (in/in);

h_{HMA} is the thickness of the HMA layer (in);

n is the number of axle-load repetitions;

T is the mix or pavement temperature (°F);

k_z is the depth confinement factor;

$k_{1r,2r,3r}$ are the global field calibration parameters (from the NCHRP 1-40D recalibration) ($k_{1r} = -3.35412$; $k_{2r} = 0.4791$; $k_{3r} = 1.5606$);

β_{1r}, β_{2r}, β_{3r} are the local or mixture field calibration constants; for the global calibration (these constants were all set to 1.0);

D is the depth below the surface (in);

H_{HMA} is the total HMA thickness (in).

Appendix A.1.3. Rutting in Unbound Pavement Layers and Foundation or Embankment Soil

$$\Delta_{p(soil)} = \beta_{s1} k_{s1} \varepsilon_v h_{soil} \left(\frac{\varepsilon_0}{\varepsilon_r}\right) e^{-\left(\frac{\rho}{n}\right)^{\beta}} \tag{A15}$$

$$Log\beta = -0.61119 - 0.017638(W_c) \tag{A16}$$

$$\rho = 10^9 \left(\frac{C_0}{\left(1 - (10^9)^{\beta}\right)}\right)^{\frac{1}{\beta}} \tag{A17}$$

$$C_0 = Ln\left(\frac{a_1 M_r^{b_1}}{a_9 M_r^{b_9}}\right) = 0.0075 \tag{A18}$$

where

$\Delta_{p(soil)}$ is the permanent or plastic deformation for the layer (in);

n is the number of axle-load applications;

ε_0 is the intercept determined from the laboratory repeated load permanent deformation tests (in/in);

ε_r is the resilient strain imposed in the laboratory tests to obtain the material properties ε_0, ε, and ρ (in/in);

ε_v is the average vertical resilient or elastic strain in the layer and calculated by the structural response model (in/in);

h_{soil} is the thickness of the unbound layer (in);

k_{s1} are the global calibration coefficients: $k_{s1} = 1.673$ for granular materials and $k_{s1} = 1.35$ for fine-grained materials;

ε_{s1} is the local calibration constant for the rutting in the unbound layers—the local calibration constant was set to 1.0 for the global calibration effort;

W_c is the water content (%);

M_r is the resilient modulus of an unbound layer (psi);

$a_{1,9}$ are regression constants: $a_1 = 0.15$; $a_9 = 20.0$;

$b_{1,9}$ are regression constants: $b_1 = 0.0$; $b_9 = 0.0$.

Appendix A.1.4. International Roughness Index (IRI)

$$IRI = IRI_0 + 0.0150(SF) + 0.400(FC_{Total}) + 0.0080(TC) + 40.0(RD) \quad \text{(A19)}$$

$$SF = Age[0.02003(PI+1) + 0.007947(PR+1) + 0.000636(FI+1)] \quad \text{(A20)}$$

where

IRI_0 is the initial IRI after construction (in/mi);

SF is the site factor;

FC_{Total} is the area of fatigue cracking (combined alligator, longitudinal, and reflection cracking in the wheel path), percent of total lane area; all load cracks are combined on an area basis—the length of cracks is multiplied by 1 ft to convert length into an area basis;

TC is the length of transverse cracking, including the reflection of the transverse cracks in existing HMA pavements (ft/mi);

RD is the average rut depth (in);

Age is the pavement age (years);

PI is the percent of the plasticity index of the soil;

FI is the average annual freezing index (°F days);

PR is the average annual precipitation or rainfall (in).

Transverse cracking-thermal cracking

$$\Delta C = A(\Delta K)^n \quad \text{(A21)}$$

$$A = 10^{k_t \beta_t (4.389 - 2.52 Log(E_{HMA} \sigma_m n))} \quad \text{(A22)}$$

$$\eta = 0.8\left[1 + \frac{1}{m}\right] \quad \text{(A23)}$$

$$K = \sigma_{tip}\left[0.45 + 1.99(C_0)^{0.56}\right] \quad \text{(A24)}$$

$$TC = \beta_{t1} N\left[\frac{1}{\sigma_d} Log\left(\frac{C_d}{H_{HMA}}\right)\right] \quad \text{(A25)}$$

where

ΔC is the change in the crack depth due to a cooling cycle;

ΔK is the change in the stress intensity factor due to a cooling cycle;

A, n are the fracture parameters for the HMA mixture;

k_t is the coefficient determined through global calibration for each input level (level 1 = 5.0; level 2 = 1.5; and level 3 = 3.0);

E_{HMA} is the HMA indirect tensile modulus (psi);

σ_m is the mixture tensile strength (psi);

m is the m-value derived from the indirect tensile creep compliance curve measured in the laboratory;

β_t is the local or mixture calibration factor;

σ_{tip} is the far-field stress from the pavement response model at the depth of the crack tip (psi);

C_0 is the current crack length (ft);

TC is the observed amount of thermal cracking (ft/mi);

β_{t1} is the regression coefficient determined through global calibration (400);

$N[z]$ is the standard normal distribution evaluated at $[z]$;

σ_d is the standard deviation of the log of the depth of cracks in the pavement (0.769) (in);

C_d is the crack depth (in);

H_{HMA} is the thickness of the HMA Layers (in).

Reflection cracking

$$RC = \frac{100}{1 + e^{a(c)+bt(d)}} \tag{A26}$$

$$a = 3.5 + 0.75 \times (H_{eff}) \tag{A27}$$

$$b = -0.688684 - 3.37302 \times (H_{eff})^{-0.915469} \tag{A28}$$

where

RC is the percent of cracks reflected; the percent of the area of reflection cracking is output with the width of cracks being 1 ft;

t is the time (years);

a, b are regression fitting parameters defined through the calibration process;

c, d are user-defined cracking progression parameters;

H_{eff} is the thickness of HMA layers in new flexible pavements (in).

References

1. Pérez-Acebo, H.; Linares-Unamunzaga, A.; Abejón, R.; Rojí, E. Research Trends in Pavement Management during the First Years of the 21st Century: A Bibliometric Analysis during the 2000–2013 Period. *Appl. Sci.* **2018**, *8*, 1041. [CrossRef]
2. AASHTO. *Guide for Design of Pavement Structures*, 4th ed.; American Association of State Highway and Transportation Officials: Washington, DC, USA, 1993; pp. 1–640.
3. AASHTO. *Mechanistic-Empirical Pavement Design Guide—A Manual of Practice*, 1st ed.; American Association of State Highway and Transportation Officials: Washington, DC, USA, 2008; pp. 1–204.
4. Ng, K.; Hutson, Z.; Ksaibati, K.; Wulff, S. A comprehensive field and laboratory test programme and electronic database of pavement material properties for MEPDG. *Int. J. Pavement Eng.* **2019**, *20*, 600–614. [CrossRef]
5. AASHTO. *Guide for the Local Calibration of the Mechanical-Empirical Pavement Design Guide*; American Association of State Highway and Transportation Officials: Washington, DC, USA, 2010; pp. 1–211. Available online: http://aii.transportation.org/Documents/LCG-1rev3lo-res.pdf (accessed on 3 January 2020).
6. Walubita, L.; Lee, S.; Faruk, A.; Hoeffner, J.; Scullion, T.; Abdallah, I.; Nazarian, S. *Texas Flexible Pavements and Overlays: Calibration Plans for m-e Models and Related Software*; Report No. FHWA/TX-13/0-6658-P4; Center for Transportation Infrastructure Systems, the University of Texas at El Paso: El Paso, TX, USA, 2013; pp. 1–146. Available online: https://static.tti.tamu.edu/tti.tamu.edu/documents/0-6658-P4.pdf (accessed on 3 January 2020).
7. Jannat, G.; Yuan, X.; Shehata, M. Development of regression equations for local calibration of rutting and IRI as predicted by the MEPDG models for flexible pavements using Ontario's long-term PMS data. *Int. J. Pavement Eng.* **2016**, *17*, 166–175. [CrossRef]
8. Jannat, G.; Tighe, S. An experimental design-based evaluation of sensitivities of MEPDG prediction: Investigating main and interaction effects. *Int. J. Pavement Eng.* **2016**, *17*, 615–625. [CrossRef]
9. Saha, J.; Nassiri, S.; Soleymani, H.; Bayat, A. A comparative study between Alberta transportation flexible pavement design and MEPDG. *Int. J. Pavement Res. Technol.* **2012**, *5*, 379–385. Available online: http://www.ijprt.org.tw/reader/pdf.php?id=263 (accessed on 4 January 2020).
10. Saha, J.; Nassiri, S.; Bayat, A.; Soleymani, H. Evaluation of the effects of Canadian climate conditions on the MEPDG predictions for flexible pavement performance. *Int. J. Pavement Eng.* **2014**, *15*, 392–401. [CrossRef]
11. Nassiri, S.; Bayat, A.; Kilburn, P. Traffic inputs for mechanistic-empirical pavement design guide using weigh-in-motion systems in Alberta. *Int. J. Pavement Eng.* **2014**, *15*, 483–494. [CrossRef]
12. El-Badawy, S.; Bayomy, F.; Fugit, S. Traffic characteristics and their impact on pavement performance for the implementation of the Mechanistic-Empirical Pavement Design Guide in Idaho. *Int. J. Pavement Res. Technol.* **2012**, *5*, 386–394. Available online: http://www.ijprt.org.tw/reader/pdf.php?id=264 (accessed on 4 January 2020).

13. Wu, Z.; Yang, X.; Zhang, Z. Evaluation of MEPDG flexible pavement design using pavement management system data: Louisiana experience. *Int. J. Pavement Eng.* **2013**, *14*, 674–685. [CrossRef]
14. Hasan, M.R.M.; Hiller, J.; You, Z. Effects of mean annual temperature and mean annual precipitation on the performance of flexible pavement using ME design. *Int. J. Pavement Eng.* **2016**, *17*, 647–658. [CrossRef]
15. Wang, Y.; Leng, Z.; Wang, G. Structural contribution of open-graded friction course mixes in mechanistic-empirical pavement design. *Int. J. Pavement Eng.* **2014**, *15*, 731–741. [CrossRef]
16. Breakah, T.; Bausano, J.; Williams, R.; Vitton, S. The impact of fine aggregate characteristics on asphalt concrete pavement design life. *Int. J. Pavement Eng.* **2011**, *12*, 101–109. [CrossRef]
17. Li, Q.; Wang, K.; Hall, K. Verification of virtual climatic data in MEPDG using the LTPP Database. *Int. J. Pavement Res. Technol.* **2010**, *3*, 10–15. Available online: http://www.ijprt.org.tw/reader/pdf.php?id=83 (accessed on 5 January 2020).
18. Plescan, C.; Plescan, E.-L.; Stanciu, M.; Botis, M.; Taus, D. Sensitivity Analysis of Rigid Pavement Design Based on Semi-Empirical Methods: Romanian Case Study. *Symmetry* **2021**, *13*, 168. [CrossRef]
19. JAE. *Manual of Pavement Structures for the Portuguese road Network*; Junta Autónoma de Estradas: Lisbon, Portugal, 1995; pp. 1–54. Available online: https://apps.uc.pt/courses/PT/unit/9167/14369/2019-2020 (accessed on 5 January 2020). (In Portuguese)
20. Walubita, L.; Fuentes, L.; Faruk, A.; Komba, I.; Prakoso, A.; Naik, B. Mechanistic-empirical compatible traffic data generation: Portable weigh-in-motion versus cluster analysis. *J. Test. Eval.* **2000**, *48*, 2377–2392. [CrossRef]
21. Oh, J.; Walubita, L.; Leidy, J. Establishment of statewide axle load spectra data using cluster analysis. *KSCE J. Civ. Eng.* **2015**, *19*, 2083–2090. [CrossRef]
22. Branco, F.; Pereira, P.; Picado-Santos, L. *Road Pavements*, 5th ed.; Almedina: Coimbra, Portugal, 2016; pp. 1–388. (In Portuguese)
23. TDOT. Available online: http://onlinemanuals.txdot.gov/txdotmanuals/tri/classifying_vehicles.htm (accessed on 5 October 2020).
24. FHWA. Available online: http://www.fhwa.dot.gov/environment/air_quality/conformity/research/improving_data/taqs03.cfm (accessed on 5 October 2020).
25. Walubita, L.; Das, G.; Espinoza, E.; Oh, J.; Scullion, T.; Lee, S.; Garibay, J.; Nazarian, S.; Abdallah, I. *Texas Flexible Pavements and Overlays: Year 1 Report—Test Sections, Data Collection, Analyses, and Data Storage System*; Report No. FHWA/TX-12/0-6658-1; Center for Transportation Infrastructure Systems, The University of Texas at El Paso: El Paso, TX, USA, 2012; pp. 1–168. Available online: https://static.tti.tamu.edu/tti.tamu.edu/documents/0-6658-1.pdf (accessed on 6 January 2020).
26. Walubita, L.; Das, G.; Espinoza, E.; Oh, J.; Scullion, T.; Nazarian, S.; Abdallah, I.; Garibay, J. *Texas Flexible Pavements and Overlays: Data Analysis Plans and Reporting Format*; Report No. FHWA/TX-11/0-6658-P3; Center for Transportation Infrastructure Systems, the University of Texas at El Paso: El Paso, TX, USA, 2012; pp. 1–136. Available online: https://static.tti.tamu.edu/tti.tamu.edu/documents/0-6658-P3.pdf (accessed on 6 January 2020).
27. Walubita, L.; Lee, S.; Faruk, A.; Scullion, T.; Nazarian, S.; Abdallah, I. *Texas Flexible Pavements and Overlays: Year 5 Report—Complete Data Documentation*; Report No. FHWA/TX-15/0-6658-3; Center for Transportation Infrastructure Systems, the University of Texas at El Paso: El Paso, TX, USA, 2017; pp. 1–106. Available online: https://static.tti.tamu.edu/tti.tamu.edu/documents/0-6658-3.pdf (accessed on 6 January 2020).
28. Ferreira, A.; Meneses, S.; Vicente, F. Pavement management system for Oliveira do Hospital, Portugal. *Proc. Inst. Civ. Eng.-Transp.* **2009**, *162*, 157–169. Available online: http://www.icevirtuallibrary.com/doi/abs/10.1680/tran.2009.162.3.157 (accessed on 7 January 2020). [CrossRef]
29. Ferreira, A.; Meneses, S.; Vicente, F. Alternative decision-aid tool for pavement management. *Proc. Inst. Civ. Eng-Transp.* **2009**, *162*, 3–17. Available online: http://www.icevirtuallibrary.com/doi/abs/10.1680/tran.2009.162.1.3 (accessed on 7 January 2020). [CrossRef]
30. Picado-Santos, L.; Ferreira, A.; Antunes, A.; Carvalheira, C.; Santos, B.; Bicho, M.; Quadrado, I.; Silvestre, S. Pavement management system for Lisbon. *Proc. Inst. Civ. Eng.-Munic. Eng.* **2004**, *157*, 157–165. Available online: http://www.icevirtuallibrary.com/doi/abs/10.1680/muen.2004.157.3.157 (accessed on 11 January 2020). [CrossRef]
31. Justo-Silva, R.; Ferreira, A. Pavement maintenance considering traffic accident costs. *Int. J. Pavement Res. Technol.* **2019**, *12*, 562–573. [CrossRef]
32. Ferreira, A.; Jesus, J.; Pinto, J. Road safety management system for Oliveira do Bairro. *Proc. Inst. Civ. Eng-Transp.* **2010**, *163*, 143–155. Available online: http://www.icevirtuallibrary.com/doi/abs/10.1680/tran.2010.163.3.143 (accessed on 13 January 2020). [CrossRef]
33. Ferreira, A.; Santos, J. Life-cycle cost analysis system for pavement management at project level: Sensitivity analysis to the discount rate. *Int. J. Pavement Eng.* **2013**, *14*, 655–673. Available online: http://www.tandfonline.com/doi/abs/10.1080/10298436.2012.719618 (accessed on 13 January 2020). [CrossRef]
34. Santos, J.; Ferreira, A. Life-cycle cost analysis for pavement management at project level. *Int. J. Pavement Eng.* **2013**, *14*, 71–84. Available online: https://www.tandfonline.com/doi/abs/10.1080/10298436.2011.618535 (accessed on 13 January 2020). [CrossRef]
35. Santos, J.; Ferreira, A. Pavement design optimisation considering costs and preventive interventions. *J. Transp. Eng.* **2012**, *138*, 911–923. Available online: https://ascelibrary.org/doi/abs/10.1061/(ASCE)TE.1943-5436.0000390 (accessed on 17 January 2020). [CrossRef]

36. Shell. *Shell Pavement Design Manual—Asphalt Pavements and Overlays for Road Traffic*, 1st ed.; Shell International Petroleum Company Ltd.: London, UK, 1978; pp. 1–42. Available online: https://openlibrary.org/books/OL14134868M/Shell_pavement_design_manual (accessed on 17 January 2020).
37. Brunton, J.; Brown, S.; Pell, P. Developments to the Nottingham analytical design method for asphalt pavements. In Proceedings of the 6th International Conference on Structural Design of Asphalt Pavements, University of Michigan, Ann Arbor, MI, USA, 13–17 July 1987; Volume 1, pp. 366–377. Available online: https://trid.trb.org/view.aspx?id=281217 (accessed on 2 February 2020).
38. Asphalt Institute. *Thickness Design: Asphalt Pavements for Highways and Streets*, 10th ed.; Asphalt Institute: Lexington, KY, USA, 2011; pp. 1–98.
39. IP. Available online: http://www.estradasdeportugal.pt/ (accessed on 5 October 2020).
40. IP. *Pavement Construction Specifications*; Estradas de Portugal, SA: Lisbon, Portugal, 2014; pp. 1–211. Available online: https://www.infraestruturasdeportugal.pt/sites/default/files/cet/14_03_set_2014.pdf (accessed on 2 February 2020). (In Portuguese)
41. MOPTC. *Portuguese Law No. 110/2009 of 18 of May, Daily of the Republic*; 1st Series; Ministry of Public Works, Transports and Communications: Lisbon, Portugal, 2009; pp. 3061–3099. Available online: http://www.utap.pt/Publicacoes_utap/110-2009.pdf (accessed on 3 February 2020). (In Portuguese)
42. Santos, J.; Ferreira, A.; Flintsch, G.; Cerezo, V. A multi-objective optimization approach for sustainable pavement management. *Struct. Infrastruct. Eng.* **2018**, *14*, 854–868. [CrossRef]